Correlated Exciton Transport in Rydberg-Dressed-Atom Spin Chains

H. Schempp,[1] G. Günter,[1] S. Wüster,[2] M. Weidemüller,[1,3] and S. Whitlock[1,*]
[1]Physikalisches Institut, Universität Heidelberg, Im Neuenheimer Feld 226, 69120 Heidelberg, Germany
[2]Max Planck Institute for the Physics of Complex Systems, Nöthnitzer Strasse 38, 01187 Dresden, Germany
[3]Hefei National Laboratory for Physical Sciences at the Microscale and Department of Modern Physics and CAS Center for Excellence and Synergetic Innovation Center in Quantum Information and Quantum Physics, University of Science and Technology of China, Hefei, Anhui 230026, China
(Received 6 April 2015; published 26 August 2015)

We investigate the transport of excitations through a chain of atoms with nonlocal dissipation introduced through coupling to additional short-lived states. The system is described by an effective spin-1/2 model where the ratio of the exchange interaction strength to the reservoir coupling strength determines the type of transport, including coherent exciton motion, incoherent hopping, and a regime in which an emergent length scale leads to a preferred hopping distance far beyond nearest neighbors. For multiple impurities, the dissipation gives rise to strong nearest-neighbor correlations and entanglement. These results highlight the importance of nontrivial dissipation, correlations, and many-body effects in recent experiments on the dipole-mediated transport of Rydberg excitations.

DOI: 10.1103/PhysRevLett.115.093002 PACS numbers: 32.80.Rm, 03.67.-a, 42.50.Gy, 87.15.hj

The transport of energy, charge, or spin is of fundamental importance in diverse settings, ranging from the operation of nanoelectronic and spintronic devices [1–4] to the dynamics of electron-hole pairs in organic semiconductors [5,6], and in natural processes such as photosynthesis [7–11]. In these systems different elementary excitations and basic transport mechanisms can give rise to very different behavior including coherent exciton motion, thermally activated diffusion, or even collective fluidlike dynamics [12]. However, understanding or exploiting these differences (e.g., for applications in photovoltaic devices) is extremely challenging, as they depend on the complex interplay between quantum statistics, coherence, confinement, disorder, and the nature of the interactions between the constituent particles. A key question is how dissipation, through the coupling to reservoirs, leads to a crossover between coherent and incoherent motion. While dissipation is usually assumed to destroy coherence, certain dissipative processes, noise, or specially structured environments may positively affect transport [7,8,10,13,14] or even preserve coherence [15], both in engineered quantum systems and in natural ones.

Here, we analyze the excitonlike motion of individual excitations through a network of dipole interacting quantum systems (i.e., atoms, molecules, or quantum dots) in the presence of a specially engineered reservoir [Fig. 1(a)]. Each subsystem is assumed to be coupled to one or more additional short-lived states. The populations of these states are determined by the coupling fields and by their proximity to any excitations, which provides a handle to introduce and control new types of dissipation in the system. By eliminating the short-lived states we show that the resulting system is characterized by coherent hopping and nonlocal dissipative terms, which lead to correlated exciton motion. Simulations of the single excitation and the two excitation dynamics demonstrate this has a dramatic effect on the transport properties, leading for example to the emergence of a new length scale for hopping and strong spatial correlations even at steady state.

As a physically realizable system we propose a chain of ultracold atoms in which Rydberg states with large transition electric dipole moments are optically coupled to

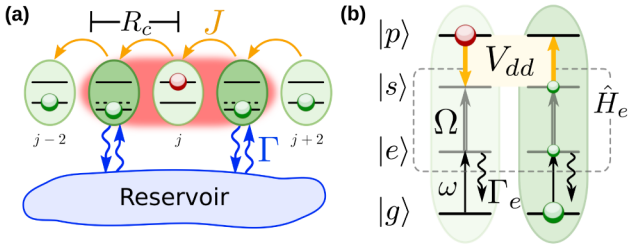

FIG. 1 (color online). Transport of excitations (red spheres) through a chain of optically dressed atoms with site index j (green spheres). (a) Excitonic motion arises through coherent long range exchange interactions J and through dissipative processes mediated by a tailored reservoir coupling. The blockade radius R_c refers to the distance over which the dipole-dipole interactions significantly affect the states of neighboring atoms. (b) Each site is represented by an atom, which can be in either the impurity Rydberg state $|p\rangle$ or the auxiliary states $|g\rangle$, $|e\rangle$, or $|s\rangle$. Dipolar interactions result in exchange between $|s\rangle$ and $|p\rangle$ Rydberg states. States $|g\rangle \leftrightarrow |e\rangle$ and $|e\rangle \leftrightarrow |s\rangle$ are coupled with Rabi frequencies ω and Ω, respectively. The state $|e\rangle$ spontaneously decays to the $|g\rangle$ state with the rate Γ_e. The state space $\hat{H}_e$ comprising $|e\rangle$ or $|s\rangle$ excitations can be adiabatically eliminated, resulting in an effective spin-1/2 model for the impurity and dressed states.

low-lying electronic states, which provides a clean synthetic system to investigate energy transfer dynamics and transport including controllable interactions and dissipation [16–27]. Recently, the excitonlike migration of an ensemble of Rydberg impurities in a bulk system was observed using electromagnetically induced transparency (EIT) of a background atomic gas as an amplifier [28]. Remarkably, the figure of merit for exciton migration, the diffusion length $L_d = \sqrt{D\tau} \approx 50$–$100\ \mu$m (with D the diffusion coefficient and τ the typical lifetime of the Rydberg state), was an order of magnitude larger than in even the purest organic semiconductors [29], and can be tuned by the probing light fields, which act as a controllable environment. In another experiment the coherent hopping of a single excitation amongst three equidistantly spaced Rydberg atoms was observed [30]. Future experiments will be able to probe the coupled coherent and incoherent motion with high spatial and temporal resolution, while the strength and nature of the dipole coupling, the degree of disorder, the excitation density, and the role of the environment can all be controlled, allowing unprecedented opportunities to investigate the fundamental processes at play.

Consider a system of ultracold atoms initially prepared in either a Rydberg state with orbital angular momentum $l = 1$ (impurity state $|p\rangle$) or the electronic ground state $|g\rangle$. The $|g\rangle$ state is weakly optically coupled via an EIT resonance to a short-lived excited state $|e\rangle$ and an $l = 0$ Rydberg state $|s\rangle$ [Fig. 1(b)]. The $|g\rangle \rightarrow |e\rangle$ probe transition is driven with Rabi frequency ω and the $|e\rangle \rightarrow |s\rangle$ coupling transition is driven with Rabi frequency Ω with $\omega \ll \Omega$. The state $|e\rangle$ spontaneously decays to $|g\rangle$ with a rate Γ_e, while the other states are assumed to be stable on the time scale of the dynamics. Migration of the $|p\rangle$ excitations among the dressed ground state atoms occurs via the $|s\rangle$ state admixture (by $|s_j\rangle|p_k\rangle \leftrightharpoons |p_j\rangle|s_k\rangle$ exchange, with j and k the site indices) [23], while the $|e\rangle$ state admixture introduces a controllable environment [31], both of which are influenced by the competition between the EIT laser fields and the Rydberg-Rydberg interactions.

The Hamiltonian describing the system is given by ($\hbar = 1$)

$$\hat{H} = \hat{H}_0 + \sum_{j\neq k} U_{\mathrm{dd}}^{(j,k)} |s_j\rangle|p_k\rangle\langle p_j|\langle s_k|, \tag{1}$$

where $\hat{H}_0 = \frac{1}{2}\sum_j \Omega|s_j\rangle\langle e_j| + \omega|e_j\rangle\langle g_j| + \mathrm{H.c.}$ accounts for the single-atom laser couplings and $U_{\mathrm{dd}}^{(j,k)} = C_m/|x_j - x_k|^m$. Here, we mainly consider dipolar interactions corresponding to $m = 3$; however, $m = 6$ can also be realized using nonresonant van der Waals interactions between Rydberg states [32–34]. For simplicity the interaction coefficient C_m is assumed to be independent of j and k. Additionally, spontaneous decay of the intermediate excited states is included through Lindblad terms leading to the master equation for the density matrix ρ

$$\dot{\rho} = -i[\hat{H}, \rho] + \mathcal{L}[\rho], \tag{2}$$

where $\mathcal{L}[\rho] = \sum_j \hat{L}_j \rho \hat{L}_j^\dagger - \frac{1}{2}(\hat{L}_j^\dagger \hat{L}_j \rho + \rho \hat{L}_j^\dagger \hat{L}_j)$ and each of the Lindblad operators represents a single decay channel ($\hat{L}_j = \sqrt{\Gamma_e}|g_j\rangle\langle e_j|$).

Simulating the open-system dynamics for more than approximately five four-level atoms is beyond what can be readily performed using exact numerical methods (e.g., Monte Carlo wave-function techniques). However, in the weak probe regime most relevant to experiments ($\omega \ll \Omega, \Gamma_e$) the populations of the $|e\rangle$ and $|s\rangle$ states are always small. Furthermore, the dynamics between these states due to the laser coupling is fast compared to the hopping dynamics. Therefore, the many-body states which include $|e\rangle$ or $|s\rangle$ can be adiabatically eliminated [35–37].

For this we use the effective operator approach, which allows for a simple interpretation of the dominant processes in terms of coherent and incoherent coupling rates (for a comprehensive description of the method see the original paper by Reiter and Sørensen [38]). First, the state space is separated into a slowly evolving "ground-state" subspace involving only $|g\rangle, |p\rangle$ states and a rapidly evolving "excited-state" subspace including $|e\rangle, |s\rangle$ states [Fig. 1(b)]. The ground state Hamiltonian contains no direct couplings $\hat{H}_g = 0$, while the coupling laser and the dipole-dipole interactions enter the Hamiltonian for the excited state manifold $\hat{H}_e$. The matrices $\hat{V}_\pm$ (with $\hat{V}_+ = \hat{V}_-^\dagger$) describe couplings between the ground and excited subspaces due to the weak probe laser coupling and can be constructed from our Hamiltonian as detailed in Ref. [38]. The master equation governing the evolution of the ground states is then defined through the operators $\hat{H}^{\mathrm{eff}} = -\hat{V}_-\mathrm{Re}[x] + \hat{H}_g$ and $\hat{L}_j^{\mathrm{eff}} = \hat{L}_j x$, where x is the solution to the matrix equation $\hat{H}_{\mathrm{NH}} x = \hat{V}_+$ with the non-Hermitian operator $\hat{H}_{\mathrm{NH}} = \hat{H}_e - (i/2)\sum_j \hat{L}_j^\dagger \hat{L}_j$. To simulate the time evolution of the system for a given set of parameters we first numerically obtain x in order to define an effective master equation [as in Eq. (2) but using the operators $\hat{H}^{\mathrm{eff}}$ and $\hat{L}_j^{\mathrm{eff}}$], which can then be solved in the usual fashion.

Single exciton dynamics.—In the special case of a single $|p\rangle$ excitation and by neglecting beyond-second-order interactions (corresponding to couplings between states involving more than one dressed atom), the effective operator approach gives an approximate analytical expression for the N-site effective master equation, which can be expressed in terms of the following effective operators:

$$\hat{H}^{\mathrm{eff}} = \sum_{k>j} J(d_{j,k}) \hat{S}_+^k \hat{S}_-^j + \mathrm{H.c.},$$
$$\hat{L}_j^{\mathrm{eff}} = \sum_{k\neq j} i\sqrt{\gamma(d_{j,k})}\hat{S}_+^k \hat{S}_-^k - \sqrt{\Gamma(d_{j,k})}\hat{S}_+^k \hat{S}_-^j, \tag{3}$$

where $d_{j,k} = |x_j - x_k|$ and we have made use of the spin raising and lowering operators ($\hat{S}_+$ and $\hat{S}_-$, respectively, with $\hat{S}^k_+ = |p_k\rangle\langle\tilde{g}_k|$, where $|\tilde{g}\rangle$ is the dressed ground state).

The resulting effective operators involve three terms: (1) effective coherent exchange interactions $J = [KV(d_{j,k})/2 + 2V(d_{j,k})^2]$, (2) incoherent hopping $\Gamma = \{KV(d_{j,k})/[2 + 2V(d_{j,k})^2]\}$, and (3) irreversible dephasing $\gamma = \{KV(d_{j,k})^4/[1 + V(d_{j,k})^2]^2\}$ acting on each site. Here, $K = \omega^2/\Gamma_e$ and $V = (R_c/d_{j,k})^3$, where $R_c = (2\Gamma_e C_3/\Omega^2)^{1/3}$ is the dipole blockade radius [28,39]. These two parameters have simple interpretations as the two-level-atom photon scattering rate and the dipole-dipole interaction energy scaled by the EIT bandwidth, respectively. K^{-1} defines a natural time scale for the dynamics whereas $V(d_{j,k})$ is responsible for the competition between coherent exchange, hopping, and dephasing. Equations (3) can be used to efficiently simulate the open-quantum-system dynamics of a single impurity immersed in a background of hundreds of optically dressed atoms in arbitrary geometries. It is interesting to note that this effective model is closely related to the widely used Haken-Strobl-Reineker (HSR) model for exciton motion in the presence of noise [40,41], including two distinct decoherence mechanisms that originate from the spontaneous decay of the $|e\rangle$ states. However, the incoherent hopping jump operators have an unusual form, $\sum_k \alpha_{j,k}\hat{S}^k_+\hat{S}^j_-$, describing correlated jumps from states $|p_j\rangle$ to collective states involving many neighboring sites k [37]. This is in contrast to the original HSR model, which ignores the influence of the system on the reservoir and assumes uncorrelated fluctuations, e.g., $\hat{L}^{\mathrm{HSR}}_{j,k} = \alpha_{j,k}\hat{S}^k_+\hat{S}^j_-$. Therefore, the system studied here offers the possibility to use dissipation controlled via EIT resonances to control both the strength and nature of decoherence in these systems, which, for example, is an active ingredient of proposals for dissipative quantum dynamics [42–46] and quantum state preparation by reservoir engineering [47–52].

Figure 2(a) shows the rates for coherent exchange, hopping, and dephasing terms as a function of the relative distance between two sites. For short distances coherent exchange is suppressed while at large distances it is determined by the $d^{-3}_{j,k}$ dependence of the dipolar interaction $J \approx (\omega^2/\Omega^2)U_{\mathrm{dd}}$. The peak exchange rate occurs for $d_{j,k} = R_c$, where $J = K/4$. At this distance, however, incoherent hopping and irreversible dephasing are equally important. For $d_{j,k} \to 0$ dephasing dominates, saturating at a rate given by the two-level-atom scattering rate $\gamma = K$.

We now turn to the analysis of spin dynamics in this system for the case of atoms arranged in a one-dimensional chain with intersite separation a (as can be produced, for example, in an optical lattice). We anticipate three main regimes: (1) for $V(a) \ll 1$ coherent exchange dominates over decoherence, (2) for $V(a) \approx 1$ decoherence becomes important leading to classical hopping, and (3) for $V(a) \gg 1$ strong dephasing suppresses coherent exchange, leaving incoherent hopping with a characteristic hopping distance comparable to R_c. Simulations for a single impurity for $N = 121$ sites are shown in Figs. 2(b)–2(e). The strength of the dipolar interactions is varied through the nearest-neighbor Rydberg-Rydberg interaction coefficient $V(a) = R^3_c/a^3$. We calculate the impurity probability distribution $P_j(t) = \mathrm{Tr}(\hat{n}_j\rho(x_j, t))$ (where $\hat{n}_j = S^j_+\hat{S}^j_-$) on each site for different values of $V(a)$.

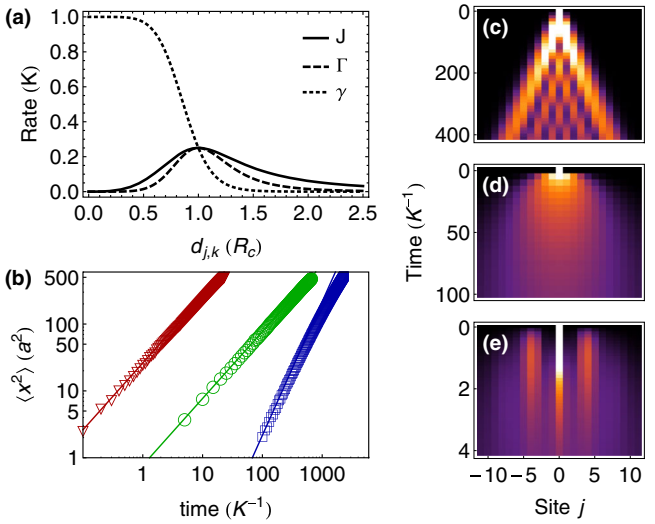

FIG. 2 (color online). (a) Distance dependence of the effective coupling rates J (solid line), Γ (dashed line), and γ (dotted line) for a single impurity with $m = 3$ in units of the two-level-atom scattering rate $K = \omega^2/\Gamma_e$. (b) Mean square displacement of the propagating excitation $\langle x^2\rangle$ for a chain of $N = 121$ sites obtained from simulations for three values of the dimensionless interaction strength: $V(a) = R^3_c/a^3 = 50$ (triangles), $V(a) = 1$ (circles), and $V(a) = 0.02$ (squares). The solid lines show the approximate analytic scalings in the three regimes described in the text. (c)–(e) Enlarged density plots showing the impurity probability distribution at short times for (c) coherent transport with $V(a) = 0.02$, (d) diffusive transport with $V(a) = 1$, and (e) transport in the blockade regime $V(a) = 50$. Bright colors indicate high probability density.

For $V(a) \ll 1$ the dynamics are characteristic of a quantum random walk, with light-cone-like spreading and interference fringes in the spatial density distribution [Fig. 2(c)]. In this regime coherent dipolar exchange dominates leading to ballistic expansion of the wave packet. For short times $t \lesssim \Gamma(a)^{-1}$ the mean square displacement (including beyond-nearest-neighbor exchange) evolves according to $\langle x^2\rangle/a^2 \approx (\pi^4/180)V(a)^2K^2t^2$ [Fig. 2(b)] [53]. For intermediate interactions [$V(a) \approx 1$] the coupled coherent and incoherent motion makes the dynamics more difficult to describe; however, from our simulations we find normal diffusion [Fig. 2(d)] with

$\langle x^2\rangle/a^2 = 2Dt$, where the diffusion coefficient $D \approx [0.262 + 0.123V(a)]K$ is found by expanding around $V(a) \approx 1$. For $V(a) \gg 1$ qualitatively new behavior is observed. We understand this as follows. For small separations between the impurity and a dressed ground state atom, the dipole-dipole interaction dominates all other coupling strengths, giving rise to delocalized excitonic eigenstates split by an energy gap $U_{\rm dd}$. This splitting breaks the two-photon (EIT) resonance condition for the dressing lasers, thereby suppressing the $|s\rangle$ state population and increasing the $|e\rangle$ state population. In the effective operator picture, this corresponds to a reduction of the coherent exchange rate at short distances (due to the reduced $|s\rangle$ state admixture) and enhanced decoherence (due to more spontaneous decay), as shown in Fig. 2(a). For another atom situated further away from the impurity, the EIT bandwidth is comparable to, or exceeds, the dipole-dipole interactions and the $|s\rangle$ state population approaches its maximum. This causes the coherent exchange rate to peak at these larger distances, accompanied by strong dephasing due to the atoms closer to the impurity. As a result incoherent transport dominates with hopping rates according to Γ, which has a preferred hopping distance given by the Rydberg blockade radius $R_c \gg a$ [Figs. 2(a) and 2(e)]. This is in contrast to the intermediate regime $V(a) \approx 1$ in which the characteristic hopping distance is set by the nearest-neighbor distance. In the strongly interacting regime the underlying lattice geometry becomes less important, leading for example to a reduced influence of possible disorder in the atomic positions. An expression for the mean square displacement can be found by neglecting coherent exchange and integrating the incoherent hopping rate for all other sites $\langle x^2\rangle/a^2 = (\pi/6)V(a)Kt$. This scaling differs from the simple picture reported in Ref. [28], where continuous observation of the system via EIT was assumed to lead to a Zeno-like slowdown of the dynamics. Instead, we demonstrate that the system exhibits a more complex form of dissipation, which allows for rapid transport even in the strongly dissipative limit.

Exciton-exciton correlations.—For times that are long compared to the inverse dissipation rate, each of the different regimes described in Fig. 2 exhibits diffusive behavior and for a finite system the excitation becomes uniformly distributed over the chain [Fig. 3(a)]. However, even at steady state ($\dot{\rho} = 0$) the nature of the transport may be revealed through the analysis of higher-order statistical properties. To demonstrate this, and to point out the importance of many-body effects, we present simulations of the effective master equation for two excitations, which could be experimentally prepared, for example, by tuning the excitation laser frequency to match the van der Waals interaction energy between a pair of p excitations at a well defined distance [54,55]. Time-dependent simulations for $N = 16$ sites for intermediate interaction strength are presented in Figs. 3(a) and 3(b) and solutions to the steady-state effective master equation for a chain of $N = 20$ sites with varying interaction strength (with periodic boundary conditions) are shown in Figs. 3(c) and 3(d). While the density distribution evolves similarly to the case of a single excitation [Fig. 3(a)], we observe strong density-density correlations $g^{(2)}(j,k) = c\langle\hat{n}_j\hat{n}_k\rangle/(\langle\hat{n}_j\rangle\langle\hat{n}_k\rangle)$, where the coefficient $c = (2N-2)/N$ normalizes to the case of precisely two excitations distributed over the chain in an uncorrelated manner [Fig. 3(b)]. These correlations persist even at steady state, long after the memory of the initial state is lost [Fig. 3(c)]. Figure 3(d) shows how the nearest-neighbor correlations depend on $V(a)$, exhibiting strong bunching for $V(a) \approx 1$. For both strong and weak interactions the correlations are suppressed, indicating that they arise as a consequence of the competition between dipole-mediated exchange and distance dependent dissipation provided by the optically dressed atoms. This dissipation is minimized for neighboring pairs and can be thought of as inducing an effective attraction between the impurities, similar to effects in Refs. [44,56]. These correlations vanish if the correlated jump operators of the effective master equation are replaced by operators that couple localized states alone. In the case of short-range interactions (i.e., van der Waals interactions with $m \geq 6$) these correlations become even more pronounced, and for nearest-neighbor interactions the steady state corresponds to the entangled pure state $|D\rangle = (N-1)^{-1/2}\sum_j(-1)^j|\tilde{g}_1\cdots p_j p_{j+1}\cdots\tilde{g}_N\rangle$.

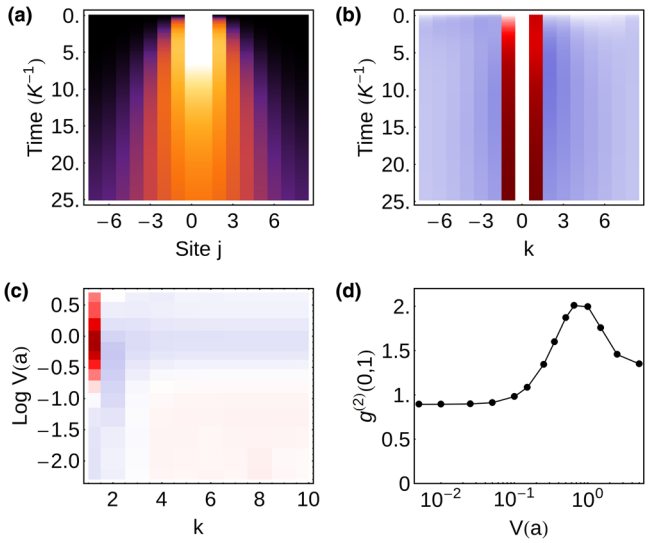

FIG. 3 (color online). Two exciton dynamics and density-density correlations $g^{(2)}$ for $\Gamma = 1$, $\Omega = 2$, $K = 0.05$, $m = 3$, and varying $V(a)$. (a) Probability density as a function of time for $V(a) = 1$ showing normal diffusion. (b) Equal time correlation function $g^{(2)}(0,k)$ for the same parameters. The colors correspond to $g^{(2)} > 1$ (dark red), $g^{(2)} < 1$ (blue), and $g^{(2)} = 1$ (white). (c) Equal time density-density correlation function at steady state as a function of $V(a)$ [same color scale as in (b)]. (d) Nearest-neighbor correlation function $g^{(2)}(0,1)$ versus $V(a)$ showing bunching around $V(a) \approx 1$.

The described impurity plus optically dressed atom system exhibits rapid spin transport controlled by a single parameter $V(a) = 2\Gamma_e C_3/(\Omega^2 a^3)$. In addition to the coherent and incoherent hopping regimes recently investigated in a related disordered system [31], we find a blockade dominated regime in which a most-likely hopping distance emerges given by the dipole blockade radius. In the limit of low impurity densities we derive an effective master equation that can be directly applied to current experiments on Rydberg energy transport in optically driven systems, helping to elucidate the interplay between coherent spin exchange and decoherence due to spontaneous decay of the dressed states. Similar physics could arise in other systems where correlated noise [57] or exciton-vibrational coupling [7,8,58,59] significantly affects transport properties. For multiple excitations we observe strong density-density correlations, which persist at steady state indicating effective interactions between excitations mediated by the nontrivial dissipation. This suggests a novel and physically realizable experimental route towards dissipative entanglement creation [47–51] and realizing exotic pairing mechanisms or exotic quantum phases in the many-body regime [60,61].

We acknowledge valuable discussions with Alexander Eisfeld, Michael Fleischhauer, Michael Höning, and Martin Rabel. This work is supported in part by the Heidelberg Center for Quantum Dynamics, the European Union H2020 FET Proactive Project RySQ (Grant No. 640378), the 7th Framework Programme Initial Training Network (COHERENCE), and the Deutsche Forschungsgemeinschaft under WH141/1-1.

*whitlock@physi.uni-heidelberg.de

[1] C. Joachim, J. Gimzewski, and A. Aviram, Nature (London) **408**, 541 (2000).
[2] A. Nitzan and M. A. Ratner, Science **300**, 1384 (2003).
[3] I. Žutić, J. Fabian, and S. Das Sarma, Rev. Mod. Phys. **76**, 323 (2004).
[4] G. Catalan, J. Seidel, R. Ramesh, and J. F. Scott, Rev. Mod. Phys. **84**, 119 (2012).
[5] G. M. Akselrod, P. B. Deotare, N. J. Thompson, J. Lee, W. A. Tisdale, M. A. Baldo, V. M. Menon, and V. Bulović, Nat. Commun. **5**, 3646 (2014).
[6] S. M. Menke and R. J. Holmes, Energy Environ. Sci. **7**, 499 (2014).
[7] T. Förster, Ann. Phys. (Berlin) **437**, 55 (1948).
[8] T. Förster, J. Biomed. Opt. **17**, 011002 (2012).
[9] H. Van Amerongen, L. Valkunas, and R. Van Grondelle, *Photosynthetic Excitons* (World Scientific, Singapore, 2000).
[10] G. D. Scholes, G. R. Fleming, A. Olaya-Castro, and R. van Grondelle, Nat. Chem. **3**, 763 (2011).
[11] E. Collini, Chem. Soc. Rev. **42**, 4932 (2013).
[12] A. Amo, D. Sanvitto, F. Laussy, D. Ballarini, E. Del Valle, M. Martin, A. Lemaitre, J. Bloch, D. Krizhanovskii, M. Skolnick *et al.*, Nature (London) **457**, 291 (2009).
[13] M. B. Plenio and S. F. Huelga, New J. Phys. **10**, 113019 (2008).
[14] F. Caruso, A. W. Chin, A. Datta, S. F. Huelga, and M. B. Plenio, J. Chem. Phys. **131**, 105106 (2009).
[15] D. Kast and J. Ankerhold, Phys. Rev. Lett. **110**, 010402 (2013).
[16] I. Mourachko, D. Comparat, F. de Tomasi, A. Fioretti, P. Nosbaum, V. M. Akulin, and P. Pillet, Phys. Rev. Lett. **80**, 253 (1998).
[17] W. R. Anderson, J. R. Veale, and T. F. Gallagher, Phys. Rev. Lett. **80**, 249 (1998).
[18] W. R. Anderson, M. P. Robinson, J. D. D. Martin, and T. F. Gallagher, Phys. Rev. A **65**, 063404 (2002).
[19] S. Westermann, T. Amthor, A. De Oliveira, J. Deiglmayr, M. Reetz-Lamour, and M. Weidemüller, Eur. Phys. J. D **40**, 37 (2006).
[20] C. S. E. van Ditzhuijzen, A. F. Koenderink, J. V. Hernández, F. Robicheaux, L. D. Noordam, and H. B. van Linden van den Heuvell, Phys. Rev. Lett. **100**, 243201 (2008).
[21] O. Mülken, A. Blumen, T. Amthor, C. Giese, M. Reetz-Lamour, and M. Weidemüller, Phys. Rev. Lett. **99**, 090601 (2007).
[22] S. Wüster, C. Ates, A. Eisfeld, and J. M. Rost, Phys. Rev. Lett. **105**, 053004 (2010).
[23] S. Wüster, C. Ates, A. Eisfeld, and J. M. Rost, New J. Phys. **13**, 073044 (2011).
[24] T. Scholak, T. Wellens, and A. Buchleitner, J. Phys. B **44**, 184012 (2011).
[25] S. Bettelli, D. Maxwell, T. Fernholz, C. S. Adams, I. Lesanovsky, and C. Ates, Phys. Rev. A **88**, 043436 (2013).
[26] F. Robicheaux and N. M. Gill, Phys. Rev. A **89**, 053429 (2014).
[27] T. Scholak, T. Wellens, and A. Buchleitner, Phys. Rev. A **90**, 063415 (2014).
[28] G. Günter, H. Schempp, M. Robert-de-Saint-Vincent, V. Gavryusev, S. Helmrich, C. S. Hofmann, S. Whitlock, and M. Weidemüller, Science **342**, 954 (2013).
[29] H. Najafov, B. Lee, Q. Zhou, L. Feldman, and V. Podzorov, Nat. Mater. **9**, 938 (2010).
[30] D. Barredo, H. Labuhn, S. Ravets, T. Lahaye, A. Browaeys, and C. S. Adams, Phys. Rev. Lett. **114**, 113002 (2015).
[31] D. W. Schönleber, A. Eisfeld, M. Genkin, S. Whitlock, and S. Wüster, Phys. Rev. Lett. **114**, 123005 (2015).
[32] D. Comparat and P. Pillet, J. Opt. Soc. Am. B **27**, A208 (2010).
[33] R. M. W. van Bijnen and T. Pohl, Phys. Rev. Lett. **114**, 243002 (2015).
[34] A. W. Glätzle, M. Dalmonte, R. Nath, C. Gross, I. Bloch, and P. Zoller, Phys. Rev. Lett. **114**, 173002 (2015).
[35] D. Petrosyan, J. Otterbach, and M. Fleischhauer, Phys. Rev. Lett. **107**, 213601 (2011).
[36] A. Carmele, B. Vogell, K. Stannigel, and P. Zoller, New J. Phys. **16**, 063042 (2014).
[37] A similar effect was also recently noted in M. Marcuzzi, J. Schick, B. Olmos, and I. Lesanovsky, J. Phys. A **47**, 482001 (2014).

[38] F. Reiter and A. S. Sørensen, Phys. Rev. A **85**, 032111 (2012).
[39] G. Günter, M. Robert-de-Saint-Vincent, H. Schempp, C. S. Hofmann, S. Whitlock, and M. Weidemüller, Phys. Rev. Lett. **108**, 013002 (2012).
[40] H. Haken and G. Strobl, Z. Phys. **262**, 135 (1973).
[41] P. Reineker, Phys. Lett. **42A**, 389 (1973).
[42] T. E. Lee, H. Häffner, and M. C. Cross, Phys. Rev. Lett. **108**, 023602 (2012).
[43] T. E. Lee and M. C. Cross, Phys. Rev. A **85**, 063822 (2012).
[44] C. Ates, B. Olmos, J. P. Garrahan, and I. Lesanovsky, Phys. Rev. A **85**, 043620 (2012).
[45] A. W. Glaetzle, R. Nath, B. Zhao, G. Pupillo, and P. Zoller, Phys. Rev. A **86**, 043403 (2012).
[46] A. V. Gorshkov, R. Nath, and T. Pohl, Phys. Rev. Lett. **110**, 153601 (2013).
[47] F. Verstraete, M. M. Wolf, and J. I. Cirac, Nat. Phys. **5**, 633 (2009).
[48] S. Diehl, A. Micheli, A. Kantian, B. Kraus, H. Büchler, and P. Zoller, Nat. Phys. **4**, 878 (2008).
[49] H. Weimer, M. Müller, I. Lesanovsky, P. Zoller, and H. P. Büchler, Nat. Phys. **6**, 382 (2010).
[50] H. Weimer, M. Müller, H. Büchler, and I. Lesanovsky, Quantum Inf. Process. **10**, 885 (2011).
[51] D. D. Bhaktavatsala Rao and K. Mølmer, Phys. Rev. Lett. **111**, 033606 (2013).
[52] M. Gärttner, S. Whitlock, D. W. Schönleber, and J. Evers, Phys. Rev. Lett. **113**, 233002 (2014).
[53] P. Reineker and R. Kühne, Phys. Rev. B **21**, 2448 (1980).
[54] T. Amthor, C. Giese, C. S. Hofmann, and M. Weidemüller, Phys. Rev. Lett. **104**, 013001 (2010).
[55] T. Weber, M. Höning, T. Niederprüm, T. Manthey, O. Thomas, V. Guarrera, M. Fleischhauer, G. Barontini, and H. Ott, Nat. Phys. **11**, 157 (2015).
[56] M. Lemeshko and H. Weimer, Nat. Commun. **4**, 2230 (2013).
[57] X. Chen and R. J. Silbey, J. Chem. Phys. **132**, 204503 (2010).
[58] J. Roden, G. Schulz, A. Eisfeld, and J. Briggs, J. Chem. Phys. **131**, 044909 (2009).
[59] M. del Rey, A. W. Chin, S. F. Huelga, and M. B. Plenio, J. Phys. Chem. Lett. **4**, 903 (2013).
[60] S. Diehl, W. Yi, A. J. Daley, and P. Zoller, Phys. Rev. Lett. **105**, 227001 (2010).
[61] S. Diehl, E. Rico, M. A. Baranov, and P. Zoller, Nat. Phys. **7**, 971 (2011).